Development of Fibrillar Morphology in Immiscible PP/PS Blends Under Shear Flow

Yuan Mei, Yajiang Huang, Yusong He, Qi Yang

College of Polymer Science and Engineering, State Key Laboratory of Polymer Materials Engineering, Sichuan University, Chengdu 610065, China

Received 31 May 2011; accepted 29 August 2011
DOI 10.1002/app.35555
Published online 7 December 2011 in Wiley Online Library (wileyonlinelibrary.com).

ABSTRACT: The formation dynamics of fibrillar morphology in dilute immiscible polypropylene (PP)/polystyrene blends under simple shear flow is investigated using optical-shear technique. Two strategies in generating fibrillar droplets under shear flow, namely temperature quench and shear jump, are studied. It is found that the shear-induced deformation of PP droplets is closely related to the total shear strain and changes of rheological properties of components during the temperature quench or shear-jump process. The shape evolution of fibrillar droplets under shear flow displays large deviation to the prediction of affine deformation theory based on Newtonian fluids and that of three deformation models, which consider the viscoelastic properties of components. The possible effect of droplet coalescence, breakup, and interfacial slip on the deviation between the experimental data and the prediction values for droplet deformation are discussed. © 2011 Wiley Periodicals, Inc. J Appl Polym Sci 124: 4838–4846, 2012

Key words: polymer blend; fibrillar structure; shear; viscoelasticity

INTRODUCTION

When an elongational flow or a shear flow is applied to a polymer blend in the melt state, the dispersed droplets within the blend will undergo large deformation and obtain a highly stretched shape (microfibrils), which could be frozen during subsequent cooling process. Microfibrillar polymer blends consisting of these microfibrils with small diameter and high aspect ratio usually possess excellent mechanical properties and have been studied extensively for the past three decades.[1] The formation and stability of a fibrillated structure during material processing results from interplay of viscous and interfacial forces and associated flow kinematics in various melt-processing techniques. Processing parameters (e.g., temperature, shear rate and flow condition, etc.) and material characteristics (e.g., viscosity ratio, interfacial tension and elasticity ratio, etc.) have their own influence on the fibrillation. Since the viscosity and elasticity ratio of polymer blends strongly depends on the melt temperature and shear rate, the fibrillar morphology can be controlled and designed by rheological properties of dispersed phase and matrix phase in the actual-processing condition. Therefore, it is of great importance to reveal the relationship between the fibrillar morphology and corresponding processing or material parameters.

The deformation of a spherical droplet under flow is closely related to two dimensionless parameters,[2,3] namely the viscosity ratio ($p = \eta_d/\eta_m$, where η_d and η_m are the viscosity of dispersed phase and matrix phase, respectively) and capillary number ($Ca = R\eta_m\gamma/\sigma$, where R is the initial radius of droplet, γ the shear rate, σ the interfacial tension). Huneault et al.[4] defined a reduced-capillary number Ca* ($Ca^* = Ca/Ca_{crit}$) to describe the deformation and breakup of a droplet, where Ca_{crit} is the critical capillary number and could be calculated as[5]:

$$\mathrm{Log}(Ca_{crit}) = -0.506 - 0.0994\,\log(p) + 0.124(\log(p))^2 - 0.115/(\log(p) - 0.6107). \quad (1)$$

The deformation criteria of a droplet under shear or elongation flow has been proposed[4]: (1) $Ca^* < 0.1$: droplets do not deform; (2) $0.1 < Ca^* < 1$: droplets can deform without breakup; (3) $1 < Ca^* < 4$: droplets deform followed by breakup (usually via the end-pinching mechanism); (4) $Ca^* > 4$: droplets deform into stable filaments, which could survive for certain times during shearing prior to their disintegration via Rayleigh instability. In general, droplets with the viscosity less or similar to that of matrix phase will facilitate the formation of fibrillar structures in blends when subjected to a high shear rate.[6–8] In the following discussion, the authors focus

Correspondence to: Y. Huang (hyj@scu.edu.cn).

on the influence of shear flow on droplet deformation, since it exists in most processing processes and can be considered systematically in well-defined flow geometries.[9]

Two strategies which involve the manipulation of viscoelastic properties and capillary number are usually adopted in generating fibrillar structures during processing. The first strategy is the adoption of a relative high shear rate during processing. Hashimoto et al.[10] showed that domains formed during spinodal decomposition of a polymer solution were elongated extremely into long strings under strong shear flow. The string diameter decreased with increasing in the shear rate and ultimately became the same order of the interface width, resulting in shear-induced homogenization. As far as immiscible-polymer blends are concerned, promoted fibrillation of dispersed phase and generation of finer fibrillar structures with large aspect ratio under higher shear rate have also been found in polypropylene (PP)/liquid crystal polymer (LCP),[11] polycarbonate (PC)/LCP[12], and poly(ethylene naphthalate)/LCP blends.[13] This shear-induced fibrillation effect is found to be more prominent in the blend when the viscosity ratio ($\eta_{droplet}/\eta_{matrix}$) is lower than 1.

The second strategy involves the changing (usually decreasing) of the temperature of polymer blends during shear flow.[14] Due to the different sensitivities of components to temperature, a variation in processing temperature will produce different viscosity ratios in the blends and thus provides an opportunity to manipulate the fibrillation behavior of blends.[12] The dynamic solidification of dispersed phase due to glass transition[9] or crystallization[15] has been demonstrated to be in favor of the improved stability of fibrillar structures against breakup during shearing. This strategy is of significance to the formation and stability of a fibrillated structure, since most of the commercial polymer blends would experience gradual cooling during the mold-filling and subsequent solidification process.

However, to our best knowledge, most previous investigations have concentrated on the effect of processing parameters on the final morphology of polymer blends. Little contribution has been devoted to the real-time formation process of the fibrillar structure during shear flow. Available reports on the deformation dynamic of droplets are mainly limited to blends suffering small-shear strain.[9,15] Up to now, no realistic prediction of the large deformation subjected to large-shear strain, such as fibrillar structures, seems to be proposed. Qualitative understanding about the properties–processing–structure correlation in such microfibrillar polymer blends is still lacking.

In this study, the deformation dynamics of dispersed phase after temperature quench and shear jump were examined, respectively, and compared under large-shear strain. A deeper understanding of the morphology evolution during temperature quench and shear jump would correlate with viscoelastic property of multicomponent blends more closely. A dilute blend consisting of commercial PP and polystyrene (PS) was chosen as a model system. The experimental results were compared with the prediction of affine deformation and that of deformation models proposed by Delaby et al.[16,17] Several possible reasons resulting in the deviation between the experimental data and the prediction value were discussed.

EXPERIMENTAL

Materials and blend preparation

PS (GP5250) with Tg of 100°C and a melt-flow index (MFI) of 7 g/10 min (ASTM D1238) was supplied by Taihua Plastic Ningbo, China. PP (T30s) with $T_m = 164.5$°C and MFI of 3 g/10 min (ASTM D1238) was purchased from Lanzhou Petrochemical, China. To facilitate the morphological observation in the optical-shear setup, a dilute blend ratio of PP/PS = 1/99 in weight was chosen. First, small amount of antioxidant 1010 (0.3 wt %) was precompounded with PP to prevent thermo-oxidative degradation. Then the obtained material (PP/antioxidant 1010) was blended with PS at a ratio of 1 wt % PP:99 wt % PS using internal mixing at 200°C for 5 min. Samples for rheological tests and morphology analysis were disks with 25 mm in diameter and 1 mm in thickness, which were prepared by compression molding at 200°C and 10 MPa.

Rheological measurements

Viscoelastic properties of components were measured using an Advance Rheology Expand System (ARES, TA instruments) equipped with a 25-mm cone-plate geometry. The shear viscosity and storage modulus of both pure components and their blends were measured, respectively, by steady and dynamic sweep experiments. Dynamic frequency sweep experiments within the range of 0.01–100 rad/s were carried out at 180, 190, 200, and 210°C, respectively. Steady rate sweep experiments were also carried out at these temperatures within the range of 0.01–10 s^{-1}. The rheological results indicate that the Cox–Merz rule holds at least within 10 s^{-1} as far as the viscosity is concerned.

Morphology observation

Shear experiments were carried out at various shear rates (0.1–0.4 s^{-1}) and temperatures (180, 190, 200,

and 210°C) using an optical-shear setup equipped with an Olympus microscope (BX 51, Japan) and a Linkam CSS-450 shear stage. This device allows us to investigate the deformation of PP droplets under well-controlled temperature and shear conditions.

Temperature quench test

The sample was placed between two quartz windows of shear cell and then the temperature was elevated to 210°C. The gap between two windows was modified to 300 μm. A high-rate preshearing at 5 s^{-1} for 400 s and a subsequent low-rate shearing at 0.1 s^{-1} for 20,000 s was applied to the blends to obtain a uniform and steady dispersion of PP phase droplets in PS. After that, a dynamic cooling process suddenly started with a cooling rate of 10°C/min while keeping shearing at $\gamma = 0.1$ s^{-1}. The cooling process was stopped when an isothermal temperature (such as 180°C) was reached. The above experiments were repeated with different quench temperature ranges (210–200°, 210–190, 210–180, 200–190, and 190–180°C) at $\gamma = 0.1$ s^{-1}.

Shear jump test

After a 20,000-s preshearing, shear experiments were carried out at various shear rates from 0.1 to 0.2, 0.3, and 0.4 s^{-1} in three different experimental temperatures (210, 200, and 190°C), respectively.

The real-time morphologies of PP droplets during deformation were recorded every several seconds by a CCD-camera and were analyzed using a home-developed image software. The number-average droplet length-diameter and deformation were computed in each case based on populations of about 25 droplets.

The interfacial tensions between PP and PS at different temperatures were determined by the deformed droplet method[18] with the optical-shear setup. The interfacial tension of PP/PS blend determined varied from 2.6 to 3 mN/m, and changed only slightly within the temperate range investigated. The result was consistent with the results of Kamal et al.,[19] which were obtained in high molecular weight PP/PS blends.

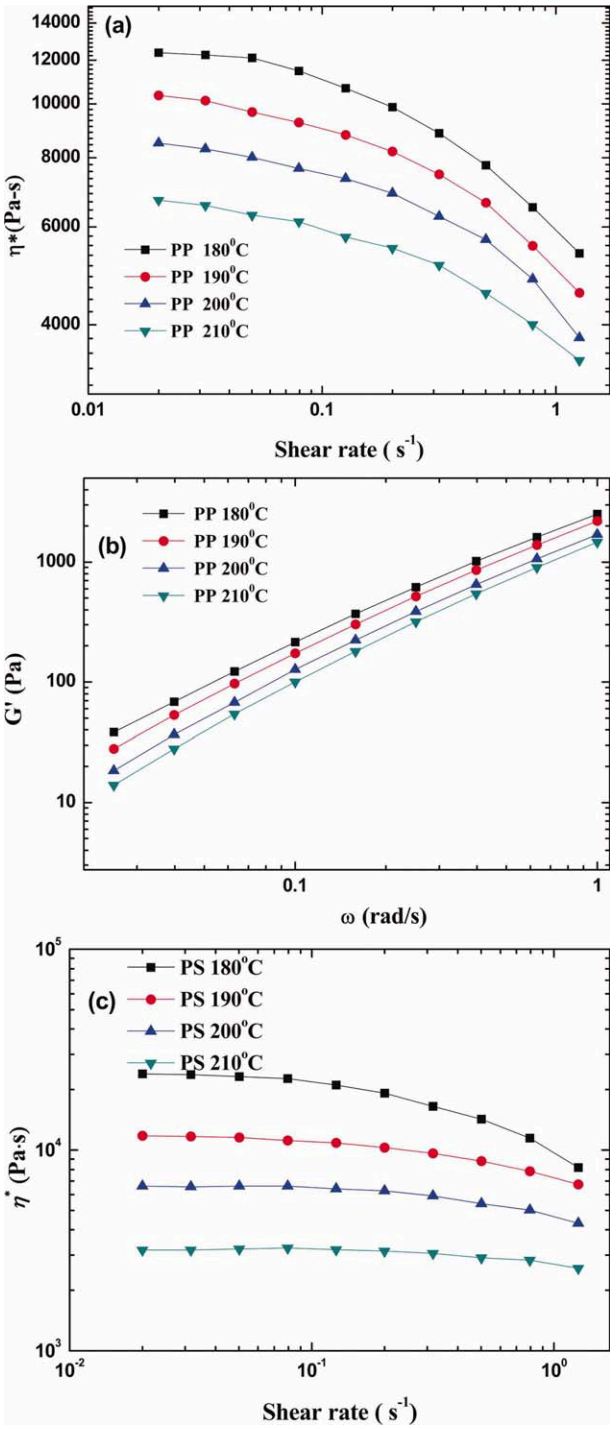

Figure 1 Viscoelastic behavior of (a) PP and (b) PS at different temperatures. [Color figure can be viewed in the online issue, which is available at wileyonlinelibrary.com.]

RESULTS AND DISCUSSION

Rheological properties

The viscoelastic properties of PP and PS were presented in Figure 1. The shear viscosity of PP and PS decreased when shear rate was increased. While the storage modulus increased with increase in shear rate. The viscosity ratio (η_d/η_m) and elasticity ratio $k = G'_d/G'_m$ (defined as the ratio of the storage modulus of components at corresponding shear rate[20]) were displayed in Figures 2 and 3, respectively. The experimental results showed that the viscosity ratio at 0.1 s^{-1} was smaller than 1.0 below 193°C and larger than 1.0 above 193°C. The viscosity ratio reduced with the decreasing of temperature and the increasing of shear rate, as shown in Figure 2. And the sensitivity of viscosity ratio to

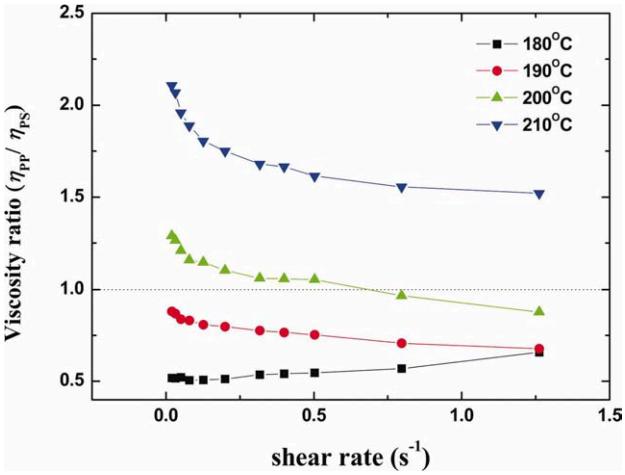

Figure 2 Shear rate dependence of viscosity ratio of PP/PS blends at different temperatures. [Color figure can be viewed in the online issue, which is available at wileyonlinelibrary.com.]

shear rate reduced with decrease in temperature. When the temperature was below 190°C, within the shear rate range considered, the viscosity ratio was always less than 1.0. Figure 3 showed the k reduced with temperature decreased and shear rate increased. The sensitivity of elasticity ratio to shear rate reduced with temperature decreased.

Development of fibrillar structure via temperature quench

The morphological evolution of PP/PS (1/99) blends after a temperature quench from 210 to 200 °C at 0.1 s^{-1} was shown in Figure 4(a). After shearing at 0.1 s^{-1} and 210°C for 20,000 s, moderated deformed PP droplets orientated in flow direction were presented in the blends. The aspect ratio of these droplets ranged from 2 to 5. The average diameter of these droplets was about 15 μm. When cooling from 210 to 200°C, the deformed PP droplets were further stretched in the flow direction accompanied by a decrease in their diameters. Long PP droplets with aspect ratio about 22 and diameter about 8 μm were found after 180 s and could survive for a long time. It was reported that a fiber droplet with aspect ratio exceeding $L/D > 10$ will undergo Rayleigh instability and disintegrate into several daughter droplets with small diameter.[21] The existence of fiber droplets with $L/D > 10$ in Figure 4 can be ascribed to the suppression effect of shear flow on the surface fluctuation of these droplets.[22–25] The confinement effect from neighbor PP fibrillar droplet may also contribute to the improved shape stability.[26] However, the disintegration of PP fibrillar droplet with diameter about 6.7 μm was still observed at $t = 480$ s. The same morphological evolution appeared in the temperature interval of 210–190 and 210–180°C, as shown in Figure 4(b,c), respectively. However, the average aspect ratio of PP fibers was the largest when cooling from 210 to 180°C. The breakup time of molten PP fibers was also the longest within the temperature quenching process from 210 to 180°C.

As shown in Figure 5, the growth rates of the average droplet aspect ratio (L/D) under different temperature ranges were basically consistent in the early time, but gave rise to large differences after 120 s. The growth rate of L/D was the fastest for the largest temperature quench depth (cooling from 210 to 180°C) while it was the slowest for the smallest temperature quench depth (i.e., from 210 to 200°C).

The effect of viscosity ratio and elasticity ratio on the fibrillar phase morphology of immiscible-polymer blends has been studied extensively in the available published reports. In general, for good fibrillation to be achieved, the viscosity of the dispersed phase had to be equal to or less than that of the matrix phase (i.e., $\eta_d/\eta_m \leq 1$).[6–8] Mighri et al.[27,28] demonstrated that matrix elasticity helped to deform the droplets, whereas the droplet elasticity resisted the droplet deformation. In Figure 5, when PP/PS blends were cooled from 210°C to different final temperatures, the difference in the rheological properties of components within 120 s was not significant. Therefore, the initial trend of three curves was basically the same. The noticeable differences between three curves after 120 s could be ascribed to the decreased viscosity ratio and elasticity ratio of blends at three different final temperatures, as demonstrated in Figures 2 and 3. These PP fibers were stable against disintegration via Rayleigh instability for certain times due to the damped interfacial disturbances by the shear flow.[22,24] Breakup of PP fibers did not occur until they were highly stretched.

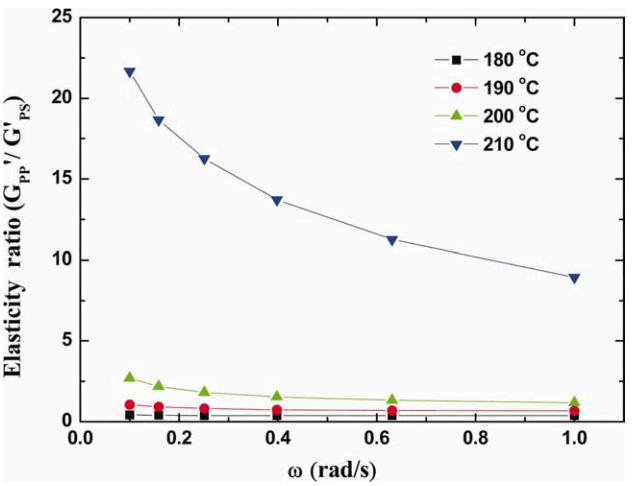

Figure 3 Shear rate dependence of elasticity ratio of PP/PS blends at different temperatures. [Color figure can be viewed in the online issue, which is available at wileyonlinelibrary.com.]

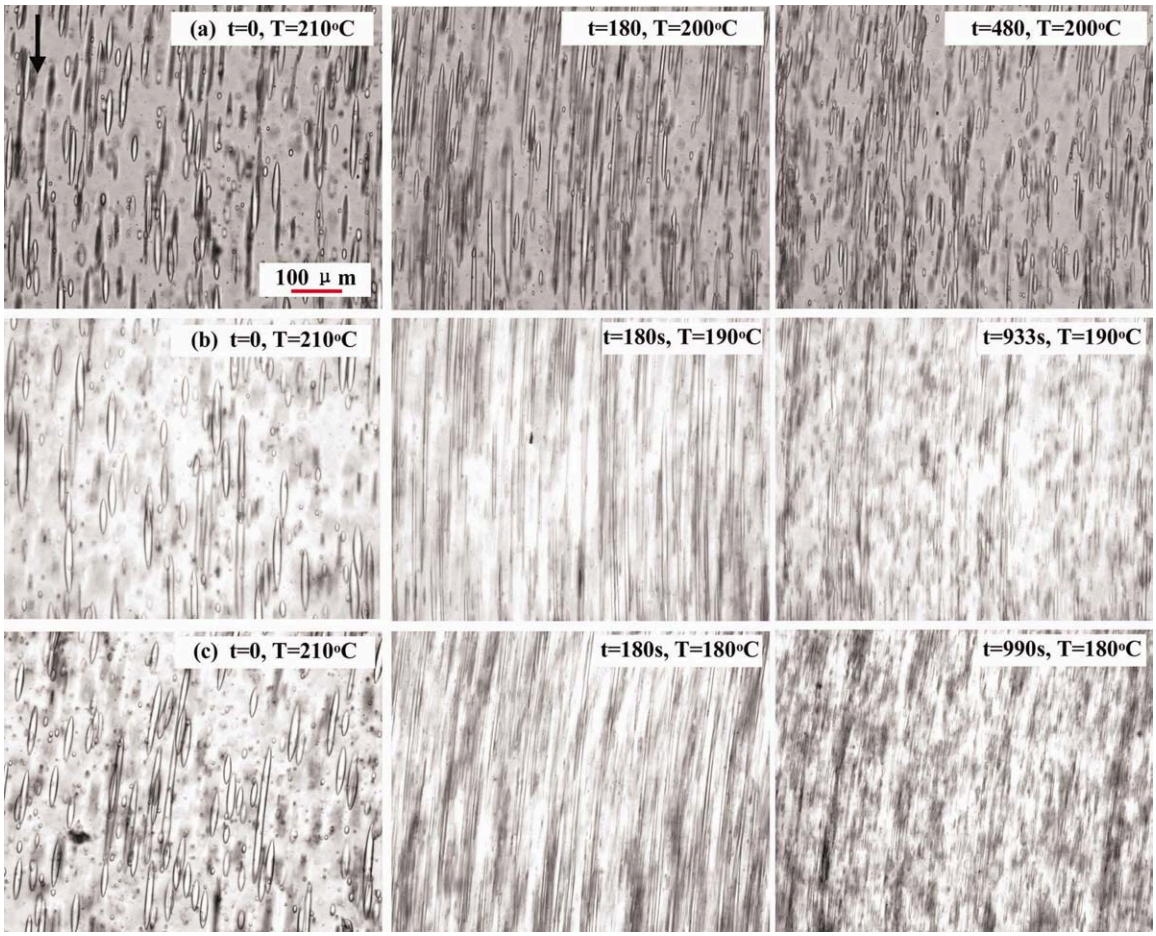

Figure 4 The morphological development of PP/PS(1/99) blends during different cooling processes: (a) 210–200°C, (b) 210–190°C, (c) 210–180°C. The scale bar denotes 100 μm. The arrows indicate the flow direction.

Figure 6 displayed the growth of the average droplet aspect ratio (*L/D*) in PP/PS blends at same quench depth but within different cooling temperature ranges at a shear rate of 0.1 s^{-1}. As shown in Figure 6, the temperature ranges were different, but the growth trends of these curves were similar. The deformation of droplet with smaller radius *R* was more difficult due to a smaller capillary number. The steady droplet radius at 210, 200, and 190°C were 14–17, 8–11, and 5–8 μm, respectively. The viscosity of PP/PS blend was the minimum when cooling from 190 to 180°C. However, the deformation rate of these droplets was significantly restricted due to their small initial droplet size. The initial size of droplets was larger at the cooling range of 210–200°C, but the viscosity ratio and elasticity ratio were higher. As a result, the trend of the three curves was basically the same.

Development of fibrillar structure via shear jump

The morphological developments of PP droplets after different shear jump processes were similar to that observed in temperature quenching process. After a sudden increase in shear rate, PP droplets in steady state were gradually stretched along the flow

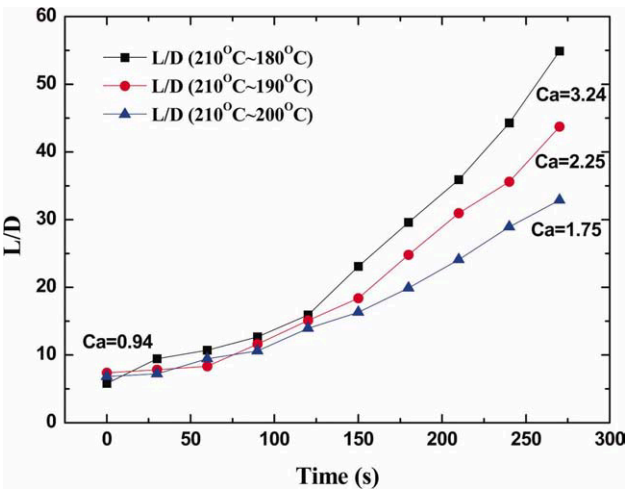

Figure 5 The aspect ratio of PP droplets versus shear time during different cooling processes at 0.1 s^{-1}. [Color figure can be viewed in the online issue, which is available at wileyonlinelibrary.com.]

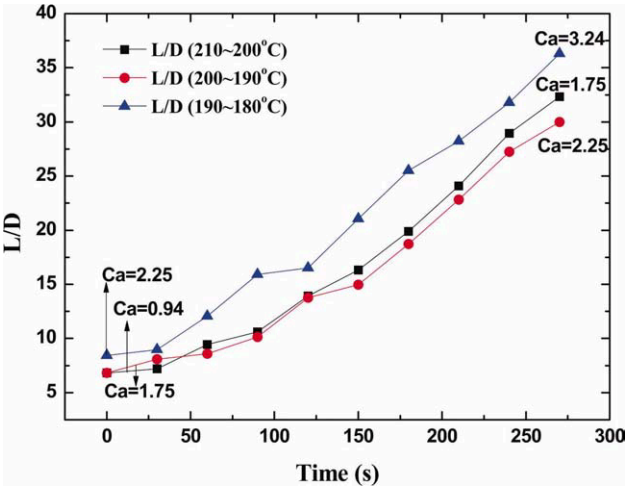

Figure 6 The average droplet aspect ratio (L/D) of PP/PS blends at same quench depth but within different cooling temperature ranges at a shear rate of 0.1 s^{-1}. [Color figure can be viewed in the online issue, which is available at wileyonlinelibrary.com.]

direction to form microfibrils. Then, long microfibrils were broken into smaller droplets via Rayleigh instability. The dependence curves of droplet deformation on matrix deformation at different ranges of shear jump were shown in Figure 7. The deformation of dispersed phase increased with shear rate. Differences in the rate of droplet deformation under different shear rates decreased with increasing temperature.

The deformation of droplet under shear flow could be predicted by the affine deformation theory[29] or three deformation models proposed by Deyrail et al.[9] According to the affine deformation theory,[29] the strain λ that really applied to a droplet, based on an affine deformation, is given by:

$$\lambda = \sqrt{1 + \gamma^2/2 + \gamma/\sqrt[2]{4 + \gamma^2}} \tag{2}$$

And the effective strain applied to the droplet is λ − 1. The droplet deformation is denoted as λ^d,

$$\lambda_d = L/L_0 \tag{3}$$

where L is the major axis of the ellipsoidal droplet and L_0 is the initial major axis of the droplet. Therefore, $\lambda_d - 1$ represents the effective deformation of droplet. On the other hand, based on the theory of droplet deformation under elongation strain proposed by Delaby et al.,[16,17] Deyrail et al.[9] derived three equations for droplet deformation of three kinds of blend systems under shear flow. Each of them takes into account relevant parameters, which affect the deformation of droplets, namely the viscosity ratio, the interfacial tension, the shear rate, the shear strain or the relaxation times of the dispersed phase, and matrix phase: (1) Model I: The

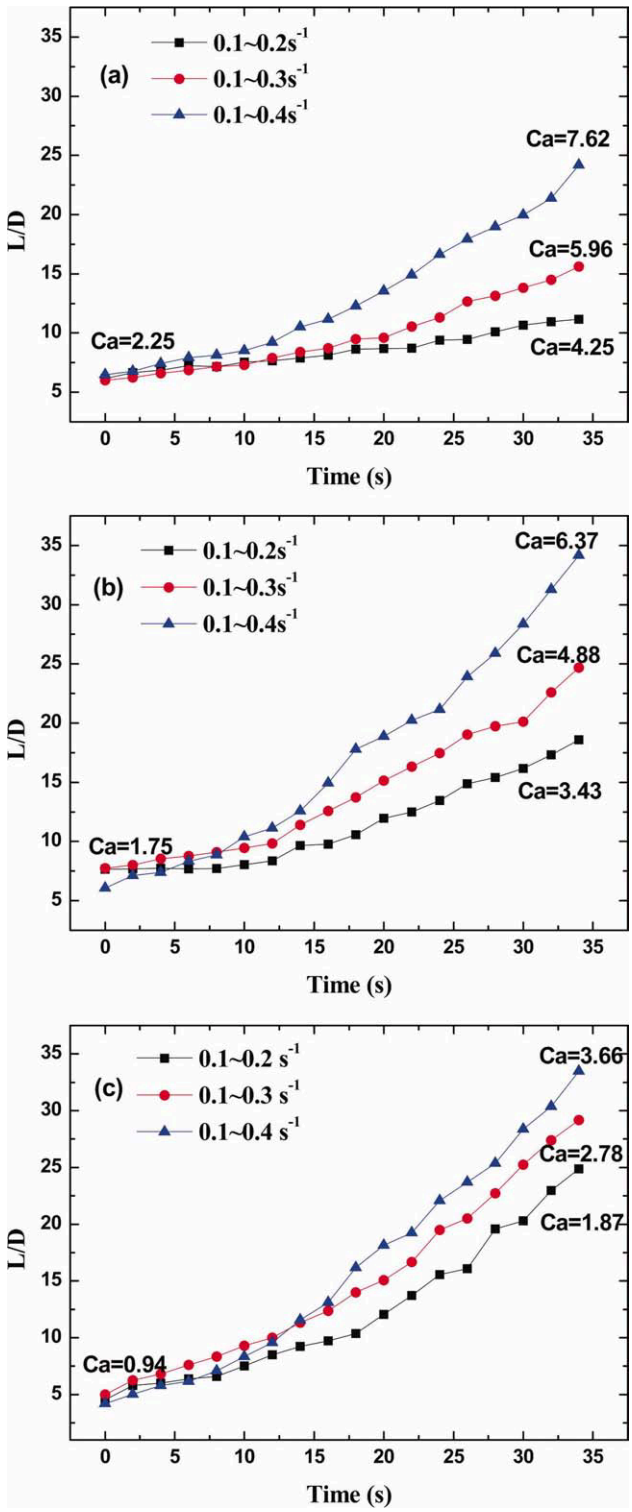

Figure 7 Droplet deformation as a function of shear time at different temperatures: (a) 190°C, (b) 200°C, (c) 210°C.[Color figure can be viewed in the online issue, which is available at wileyonlinelibrary.com.]

deformation of Newtonian phases without interfacial tension,

$$\frac{\lambda_d - 1}{\lambda - 1} = \frac{5}{2p + 3}. \quad (4)$$

(2) Model II: The deformation of Newtonian phases with interfacial tension,

$$\lambda_d - 1 = \frac{19p + 16}{16p + 16}\frac{2\gamma\eta_m R}{\sigma}\left[1 - e^{-t(20\sigma)/(R\eta_m 19p)}\right] \quad (5)$$

and (3) Model III: The viscoelastic phases without interfacial tension,

$$\lambda_d - 1 = \frac{5}{2p + 3}\gamma(t) + \frac{10p\gamma}{(2p + 3)^2}(\tau_d - \tau_m). \quad (6)$$

where σ is the interfacial tension. R represents the initial radius of droplet, p viscosity ratio, t the shear time, η_m the matrix phase viscosity. τ_d and τ_m are the relaxation time of the dispersed and the matrix. It was found that the Model I and the Model III fitted quite well with the deformation of PC droplets in ethylene-methyl acrylate copolymer (EMA) matrix under shear flow.[9]

Figure 8 shows the comparison between experimental results and the predictions of these models at 210°C. The predictions of Model I and Model III were more close to the experimental data than those of the other two models, which was consistent with the result of Deyrail et al.[9] However, on the whole, the experimental results exhibited a large negative deviation compared with prediction of these models at different ranges of shear jump. This large deviation also existed in the cases of 200 and 190°C.

The significant deviations observed may stem from several factors, including droplet dynamics (breakup and coalescence), interfacial slip between components and flow field. First, the models mentioned above were also derived based on the deformation of a single droplet under flow. However, actual blends usually consist of many dispersed droplets. Under this circumstance, the droplet–droplet interactions and dynamics of droplets (such as breakup and coalescence) may play an important role in determining the development of fibrillar structure in the blends. The droplet breakup phenomenon is controlled by the capillary number (Ca). A low Ca will result in stable and less deformed droplets.[3,30] When the viscous stress dominates the interfacial stress, i.e., with Ca larger than a critical value Ca_c, the droplets will become unstable and break.[31,32] The capillary number and critical capillary number of PP droplet in PS matrix at various temperatures and shear rates were listed in Table I. According to Table I, it was possible that droplet would break up in shear in most cases, except for the case of being sheared at 0.2 s^{-1} and

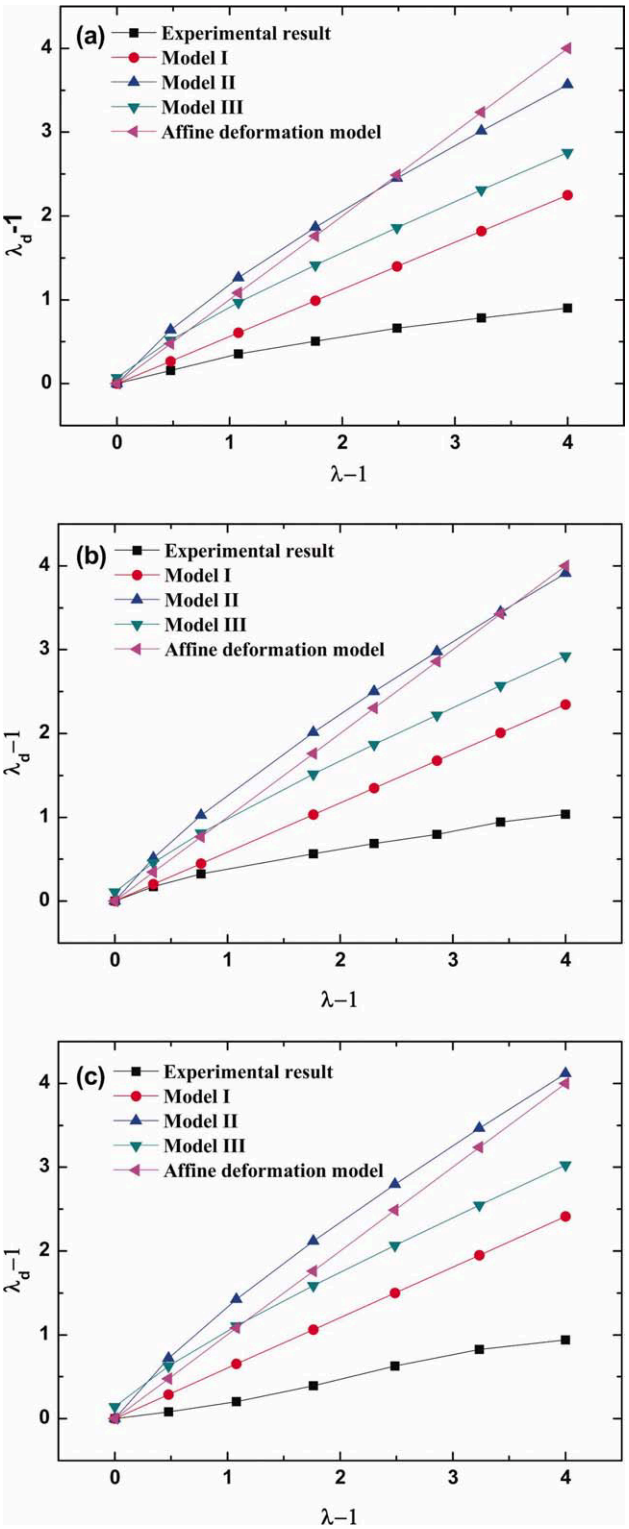

Figure 8 Droplet deformation versus matrix deformation for different ranges of shear jump at 210°C: (a) from 0.1 to 0.2 s^{-1}, (b) from 0.1 to 0.3 s^{-1}, (c) from 0.1 to 0.4 s^{-1}. [Color figure can be viewed in the online issue, which is available at wileyonlinelibrary.com.]

TABLE I
Capillary Number, Critical Capillary Number, and Reduced Capillary Number of Droplets at Various Temperatures and Shear Rates

	190°C			200°C			210°C		
Shear rate (s^{-1})	Ca	Ca_c	Ca*	Ca	Ca_c	Ca*	Ca	Ca_c	Ca*
0.1	2.25	0.47	4.83	1.75	0.55	3.20	0.94	2.55	0.37
0.2	4.25	0.46	9.15	3.43	0.53	6.41	1.87	1.94	0.96
0.3	5.96	0.46	12.86	4.88	0.53	9.15	2.78	1.43	1.95
0.4	7.62	0.46	16.46	6.37	0.52	12.28	3.66	1.21	3.02

210°C. The average volumes of droplets just after the shear jump (V_b) and 34 s after shear jump (V_e) were presented in Table II. The result in Table II indicated that the volumes of PP droplets were basically constant during the process of droplet deformation considered. Tables I and II revealed that there was a dynamic equilibrium between breakup and coalescence of droplets. The presence of breakup phenomenon would produce smaller droplets with less deformability and thus resulted in the negative deviation between the experimental and predicted values.

The existence of interfacial slip in PP/PS blends[33,34] may also influence the droplet deformation and thus contribute to the deviation observed. When subjected to shear flow, the low entanglement densities and weak interaction at interface in immiscible-polymer blends will cause the interface appears to "slip"[35] and result in negative viscosity deviation. Table III displayed the viscosity of PP/PS blends (η) and the simple additive viscosity of blends (η_a) under different temperatures and shear rates. The η_a of PP/PS blends was given by the simple additive rule,

$$\eta_a = \omega_{PP}\eta_{PP} + \omega_{PS}\eta_{PS}. \quad (7)$$

Where η_{PP} and η_{PS} are the viscosities of PP and PS, respectively. And ω_{PP} and ω_{PS} are the weight fractions of the two components. Table III showed that the negative viscosity deviation in the dilute PP/PS blends at 190, 200, and 210°C were about 6–8, 11–15, and 2–5%, respectively. The viscosity deviations are evident in these blends in regard for the low concentration of PP droplets. Due to the interfacial slip between PP droplets and PS matrix, the shear strain that actually applies to the droplets would be smaller than the strain predicted by the models. Therefore, the interfacial slip may be an important factor, which caused the negative deviation observed.

It had to be noted that all of the models reported by Delaby et al. were derived originally from the uniaxial elongational flow, which is more effective than shear flow in deforming droplets from an experimental and theoretical point of view.[11,36] Although Deyrail et al.[9] reported that the Newtonian model without interfacial tension (Model I) and the viscoelastic model (Model III) fitted quite well with the deformation of PC droplets in EMA matrix under shear flow, the applicability of these models in other polymer blends under shear flow still requires more experimental verifications.

TABLE II
The Average Volumes of Droplets at Various Temperatures and Shear Rates

	190°C		200°C		210°C	
Shear rate (s^{-1})	V_b (μm^3)	V_e (μm^3)	V_b (μm^3)	V_e (μm^3)	V_b (μm^3)	V_e (μm^3)
0.2	3396	3407	5087	5193	6061	6231
0.3	3056	3197	4939	4965	6243	6270
0.4	3286	3193	4921	4835	5935	6035

TABLE III
The Viscosity and the Simple Additive Viscosity of PP/PS Blends

	190°C		200°C		210°C	
Shear rate (s^{-1})	η_a (Pa s)	η (Pa s)	η_a (Pa s)	η (Pa s)	η_a (Pa s)	η (Pa s)
0.2	10,255	9405	6260	5319	3161	2990
0.3	9585	8947	5911	5175	3070	2922
0.4	9184	8528	5657	5029	2925	2865

CONCLUSIONS

The formation dynamics of PP microfibrils in a PP/PS (1/99) blend under simple shear flow were investigated by changing the temperature and shear rate, respectively. It has been demonstrated that a larger-quench depth in temperature facilitated the development of the PP microfibrils with higher aspect ratio due to the smaller viscosity and elasticity ratio of blends. At the same quench depth, the trend in the shape evolution of PP microfibrils at different temperatures was similar due to their differences in the initial droplet size. Differences in deformation rate of droplet under different shear rates decreased with increasing temperature. The shape development of fibrillar PP droplets under shear flow displayed large deviation both to the prediction of affine deformation theory and to that of Delaby's models, which may be ascribed to the breakup of PP droplets and the presence of interfacial slip between the droplets and the PS matrix. The applicability of Delaby's models in describing the large deformation of droplets under flow field may also require a more comprehensive evaluation.

The authors are grateful to the financial support from the National Science Foundation of China (51003062). This work was also supported in part by the Program for New Century Excellent Talents in University (NCET-10-0576), State Education Ministry, and by the State Key Laboratory of Polymer Materials Engineering of China, Sichuan University.

References

1. Li, Z.; Yang, W.; Huang, R.; Fang, X.; Yang, M. Angew Makromol Chem 2004, 289, 426.
2. Taylor, G. Proc R Soc Lond 1934, 146, 501.
3. Grace, H. Chem Eng Commun 1982, 14, 225.
4. Huneault, M.; Shi, Z.; Utracki, L. Polym Eng Sci 1995, 35, 115.
5. Debruijn Antonie, R.; Ph.D. Thesis Technische University, Eindhoven, 1991.
6. Tsebrenko, M.; Rezanova, N.; Vinogradov, G. Polym Eng Sci 2004, 20, 1023.
7. Mehta, A.; Isayev, A. Polym Eng Sci 1991, 31, 971.
8. Kim, B.; Do, I. J Appl Polym Sci 1996, 60, 2207.
9. Deyrail, Y.; Michel, A.; Cassagnau, P. Can J Chem Eng 2002, 80, 1017.
10. Hashimoto, T.; Matsuzaka, K.; Moses, E.; Onuki, A. Phys Rev Lett 1995, 74, 126.
11. Postema, A.; Fennis, P. Polymer 1997, 38, 5557.
12. Tan, L.; Yue, C.; Tam, K.; Lam, Y.; Hu, X. Polym Int 2002, 51, 398.
13. Li, L.; Chan, C.; Yue, C.; Lam, Y.; Tam, K. J Appl Polym Sci 2004, 91, 1505.
14. Martin, P.; Carreau, P. J.; Favis, B. D.; Jerome, R. J Rheol 2000, 44, 569.
15. Deyrail, Y.; Fulchiron, R.; Cassagnau, P. Polymer 2002, 43, 3311.
16. Delaby, I.; Muller, R.; Ernst, B. Rheol Acta 1995, 34, 525.
17. Delaby, I.; Ernst, B.; Froelich, D.; Muller, R. Polym Eng Sci 1996, 36, 1627.
18. Xing, P.; Bousmina, M.; Rodrigue, D.; Kamal, M. Macromolecules 2000, 33, 8020.
19. Kamal, M.; Lai-Fook, R.; Demarquette, N. Polym Eng Sci 1994, 34, 1834.
20. Levitt, L.; Macosko, C.; Pearson, S. Polym Eng Sci 1996, 36, 1647.
21. Tucker, C. L.; Moldenaers, P. Annu Rev Fluid Mech 2002, 34, 177.
22. Gunawan, A. Y.; Molenaar, J.; Van De Ven, A. A. F. Eur J Mech Fluids 2005, 24, 379.
23. Migler, K. B. Phys Rev Lett 2001, 86, 1023.
24. Frischknecht, A. Phys Rev E 1998, 58, 3495.
25. Son, Y.; Martys, N. S.; Hagedorn, J. G.; Migler, K. B. Macromolecules 2003, 36, 5825.
26. Elemans, P.; Van Wunnik, J.; Van Dam, R. Aiche J 1997, 43, 1649.
27. Mighri, F.; Ajji, A.; Carreau, P. J Rheol 1997, 41, 1183.
28. Mighri, F.; Carreau, P.; Ajji, A. J Rheol 1998, 42, 1477.
29. Elemans, P.; Bos, H.; Janssen, J.; Meijer, H. Chem Eng Sci 1993, 48, 267.
30. Bentley, B.; Leal, L. J Fluid Mech 1986, 167, 241.
31. Acrivos, A. Ann N Y Acad Sci 1983, 404, 1.
32. Rallison, J. Annu Rev Fluid Mech 1984, 16, 45.
33. Zhang, Q.; Yang, H.; Fu, Q. Polymer 2004, 45, 1913.
34. Xing, Q.; Zhu, M.; Wang, Y.; Chen, Y.; Zhang, Y.; Pionteck, J.; Adler, H. Polymer 2005, 46, 5406.
35. Jiang, L.; Lam, Y.; Yue, C.; Tam, K.; Li, L.; Hu, X. J Appl Polym Sci 2003, 89, 1464.
36. Cassagnau, P.; Deyrail, Y.; Fulchiron, R. Micro- and Nanostructured Multiphase Polymer Blend Systems: Phase Morphology and Interfaces; CRC Press: Florida, 2006; p 237.